ISSN 1070-4280, Russian Journal of Organic Chemistry, 2025, Vol. 61, No. 9, pp. 1626–1632. © Pleiades Publishing, Ltd., 2025.

Synthesis, Structure, and Properties of Acetoacetanilide Acetylhydrazone

S. Z. Sattorova[a], H. S. Aminova[a], S. F. Abdurakhmonov[a], E. A. Khudoyarova[a], B. B. Umarov[a], and Z. A. Sulaymonova[a,*]

[a] *Bukhara State University, Bukhara, 705018 Uzbekistan*

**e-mail: sulaymonovaza@mail.ru*

Received July 2, 2025; revised July 17, 2025; accepted July 18, 2025

Abstract—Acetoacetanilide acetylhydrazone has been synthesized for the first time by the condensation of acetoacetanilide with acetylhydrazide in ethanol. Its structure has been confirmed by elemental analysis, IR and UV spectra, and X-ray analysis. Thermal properties and stability of the title compound have been studied. Acetoacetanilide acetylhydrazone crystallizes in space group *P1* of the triclinic crystal system, and its stable crystal packing is determined by a system of intermolecular hydrogen bonds and possible π-stacking interactions. The obtain results suggest that compounds structurally related to acetoacetanilide acetylhydrazone are promising as ligands in coordination chemistry.

Keywords: acetylhydrazone, acetoacetanilide, crystal structure, thermal analysis

DOI: 10.1134/S1070428025603012

INTRODUCTION

Hydrazones constitute an important class of organic compounds possessing a broad range of useful chemical and biological properties. Due to the presence of a reactive C=N bond and the possibility of forming intra- and intermolecular hydrogen bonds, hydrazones are used as intermediate products in organic synthesis and ligands in coordination chemistry and are potential antimicrobial and antitumor drugs and antioxidants [1–8]. Of particular interest are hydrazones derived from acetoacetanilide which possesses an active methylene group and is capable of reacting with various nucleophiles. These hydrazones can show both interesting spectroscopic properties and biological activity.

The goal of the present work was to synthesize previously unknown acetoacetanilide acetylhydrazone, determine its molecular and crystal structure by spectroscopic methods and X-ray analysis, and study its thermal stability and biological activity.

Acetylhydrazones and their derivatives are known to exhibit pronounced antibacterial, antifungal, antitumor, and antioxidant activities [9–13]. It was found that introduction of an acetylhydrazone fragment increases the lipophilicity and cell membrane permeability of the resulting compounds, which could enhance the biological effect. Thermal stability and spectral characteristics are of particular importance among physical properties. The condensation products of acetylhydrazine are generally stable at room temperature and readily soluble in polar solvents. Their IR spectra show characteristic absorption bands due to C=O, C=N, and N–H stretching vibrations.

The presence of donor nitrogen and oxygen atoms makes acetylhydrazones potential ligands for the synthesis of transition metal complexes. Copper(II), nickel(II), and cobalt(II) chelates with acetylhydrazones coordinated in a bidentate or tridentate mode have been reported. These complexes demonstrated catalytic activity, photochemical properties, and luminescence, which expands their application scope [7–9, 11–15].

RESULTS AND DISCUSSION

The title compound, (*E*)-3-(2-acetylhydrazinylidene)-*N*-phenylbutanamide (**1a**, acetoacetanilide acetylhydrazone) was synthesized by the condensation of acetoacetanilide and acetylhydrazine (acetohydrazide) in ethanol (Scheme 1). Nucleophilic condensation of 1,3-dicarbonyl compounds, such as acetoacetanilide, with acetylhydrazine involves the acetyl group. This procedure has a number of advantages, including high

Scheme 1.

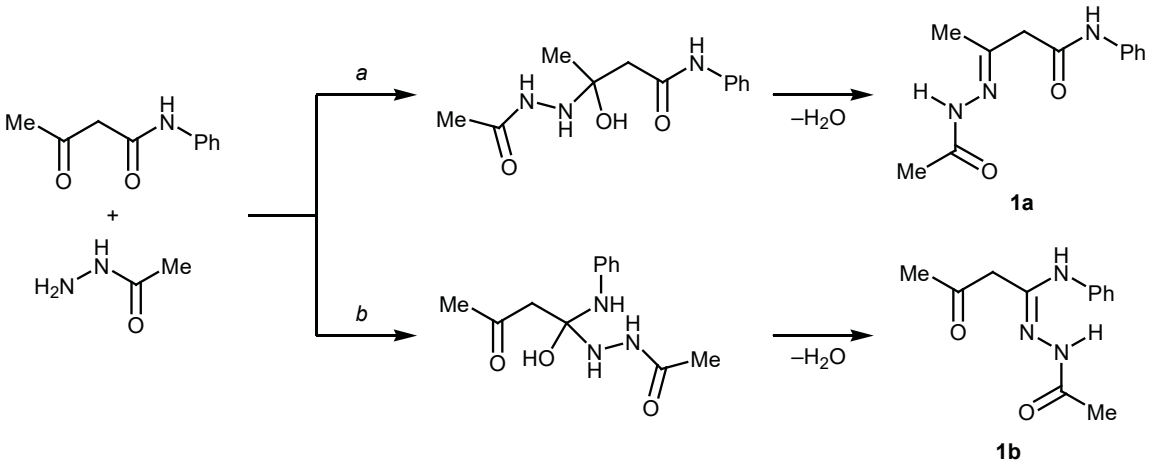

Scheme 2.

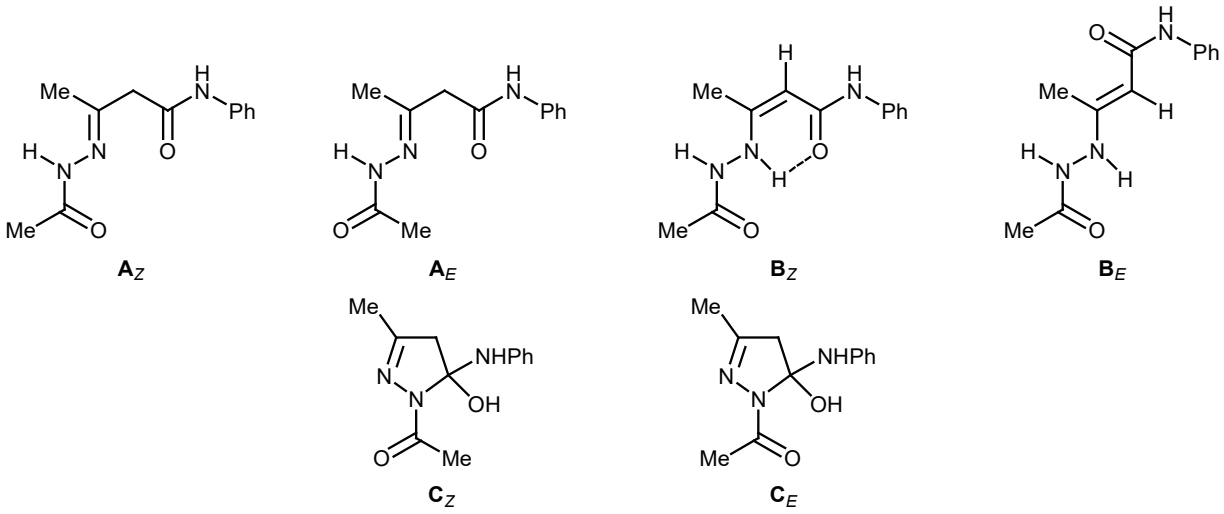

yields of ligands for the synthesis of chelate complexes and the use of available and nontoxic solvent.

Hydrazones are very prone to tautomerism, most often imine–enamine and keto–enol. According to published data, enamine or hydrazone tautomer can predominate in the solid state and in solution, depending on the solvent nature and conditions [14–16]. Acetoacetanilide acetylhydrazone can exist in several tautomeric forms, $\mathbf{A}_Z$, $\mathbf{A}_E$, $\mathbf{B}_Z$, $\mathbf{B}_E$, $\mathbf{C}_Z$, and $\mathbf{C}_E$, which differ by the position and configuration of the double bond (Scheme 2). In particular, structures denoted with the subscripts "*Z*" and "*E*" differ by configuration about the C=N bond, which is reflected in their spectral characteristics.

The morphological characteristics and element distribution in structure **1a** was studied by scanning electron microscopy (SEM), followed by EDS mapping. The SEM image of **1a** (Fig. 1) showed disordered porous surface structure with clearly observed micron-size zones. Particles of **1a** are characterized by predominantly amorphous morphology lacking distinct crystalline facets, which indicates possible aggregation and nonuniform packing density of molecules in the solid state.

Elemental analysis along the C–K, N–K, and O–K lines confirmed the presence of the corresponding elements in agreement with the proposed structure of. The distribution of carbon is uniform over the entire surface, which is typical of organic compounds. Nitrogen is also detected in all zones, through with lower intensity, which may be associated with the localization of hydrazone and amino groups. The presence of oxygen is confirmed by a weak but stable signal, especially in zones corresponding to acetyl and carbonyl groups.

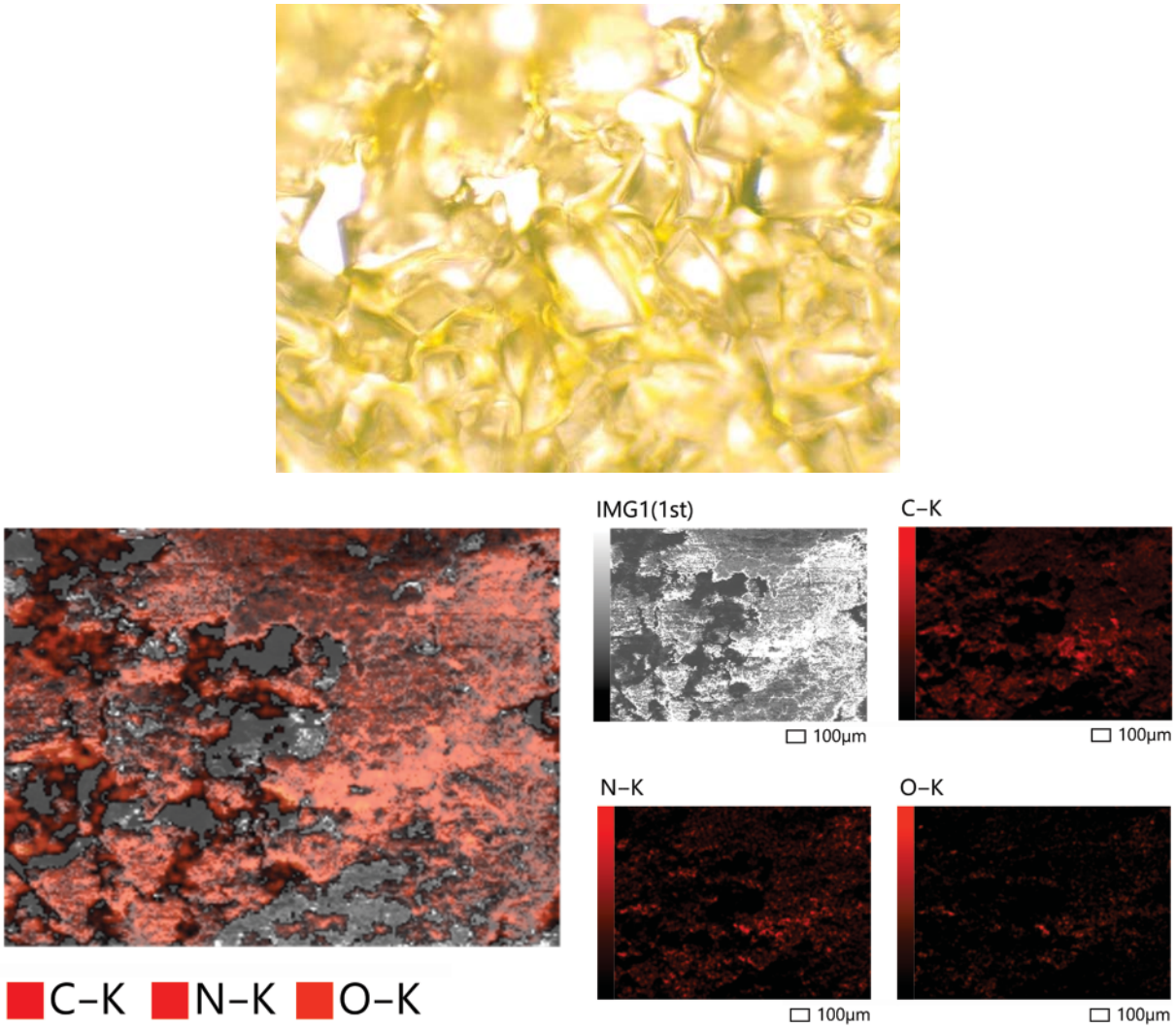

Fig. 1. SEM images of single crystals of (*E*)-3-(2-acetylhydrazinylidene)-*N*-phenylbutanamide (**1a**).

The results of SEM analysis and EDS mapping (Figs. 1, 2) suggest a uniform chemical composition of the sample surface without foreign inclusions or impurities, which confirmed the purity of the synthesized compound and uniform distribution of main functional groups at a microstructure level.

Figure 3 shows the IR spectrum of acetoacetanilide acetylhydrazone (**1a**). Stretching vibrations of the acetyl and amide carbonyl groups were observed in the region of 1710–1660 cm^{-1}. Symmetrical stretching vibration band typical of the >C=C< fragment was present at 965 cm^{-1}. Medium-intensity peaks in the region of 1400–1200 cm^{-1} were assigned to C–H_{aliph} bending vibrations and C–N stretching vibrations of the hydrazone and amide fragments. Several distinct peaks in the range of 1450–1600 cm^{-1} corresponded to stretching vibrations of C=C_{arom} and C=N bonds and bending vibrations of N–H bonds. Acetylhydrazones are generally characterized by a low-frequency shift of the C=O band due to conjugation with the C=N bond. In addition, a contribution of C=N vibrations is possible in that region (~1630–1600 cm^{-1}). Weak peaks due to stretching vibrations of aliphatic C–H bonds (CH_3 and CH_2 groups) were observed in the region of 2950–2850 cm^{-1}. Aromatic C–H stretching vibrations appeared as weak or medium-intensity peaks (or poorly resolved shoulders) appeared at 3100–3000 cm^{-1}. The hydrazone N–H stretching band was broadened as a result of hydrogen bonding.

According to the IR data, compound **1a** in the solid state has mainly acyclic hydrazone structure. For comparison, a theoretical IR spectrum of **1a** was simulated using Gaussian [17] and Avogadro [18]. The experimental IR spectrum indicated the presence of C=O and

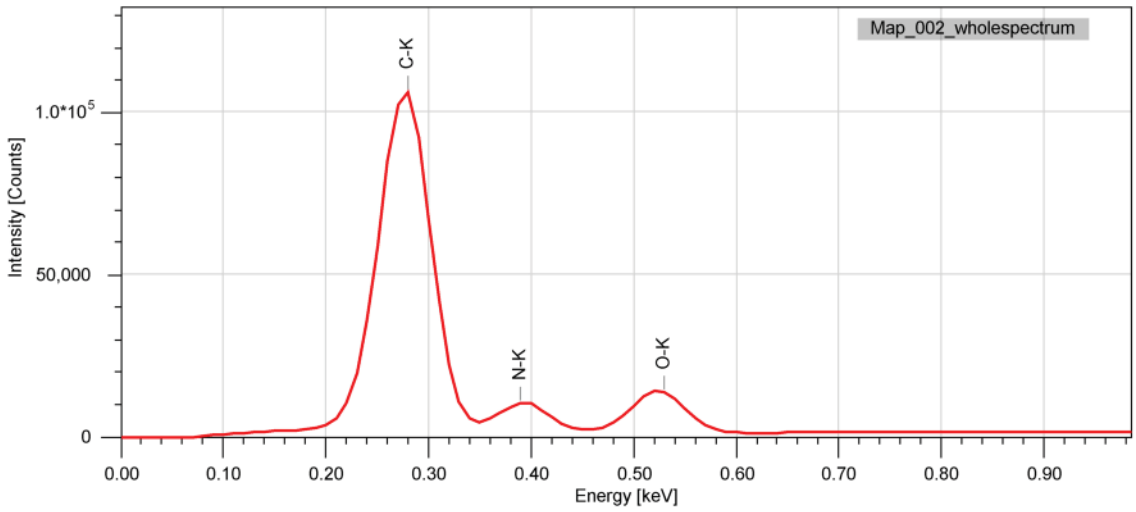

Fig. 2. EDS spectrum of compound **1a**.

C=N groups typical of acetylhydrazones. The N–H group gave rise to a broad band around 3300 cm^{-1}. In addition, bands corresponding to vibrations of aromatic ring were observed. These fundings suggest formation of a conjugated C=N/C=O bond system characteristic of hydrazone derivatives.

The electronic absorption spectrum of compound **1a** in the region of λ 300–800 nm is shown in Fig. 4. The spectrum showed a strong absorption band with its maximum at λ ~315 nm, which corresponds to π→π* and *n*→π* transitions in the aromatic and azomethine fragments. This band confirms the existence of conjugation system including the phenyl ring and hydrazone and amide groups. The lack of absorption in the visible region of the spectrum indicates the absence of strong donor–acceptor interactions, which is consistent with the proposed structure and colorlessness of compound **1a**.

Thermogravimetric analysis (TGA) of compound (**1a**) showed that its decomposition occurs in two steps. The first stage (120–230°C) corresponds to removal of physically adsorbed water or solvent residues, as well as of weakly bound molecules; at this stage, the weight loss is ~1 mg. The compound is thermally stable to ~200°C. The second stage is main decomposition of the carbon skeleton in the temperature range 230–350°C, which is accompanied by a sharp weight loss. This stage involves rupture of C=N, C=O, and C–N

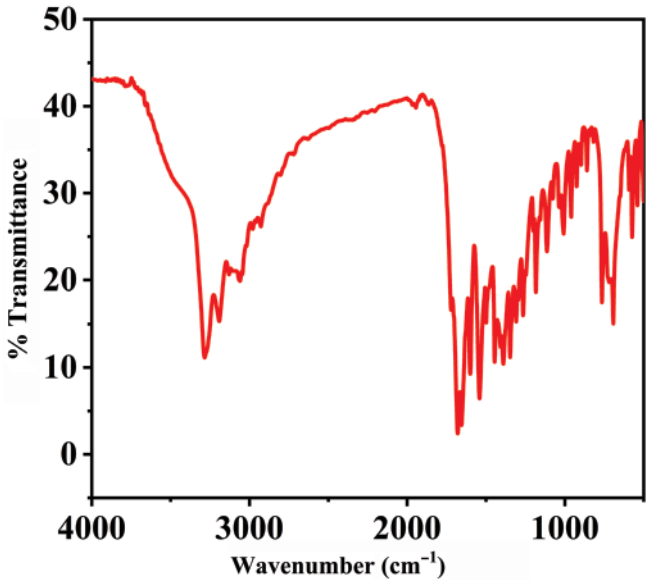

Fig. 3. IR spectrum of compound **1a**.

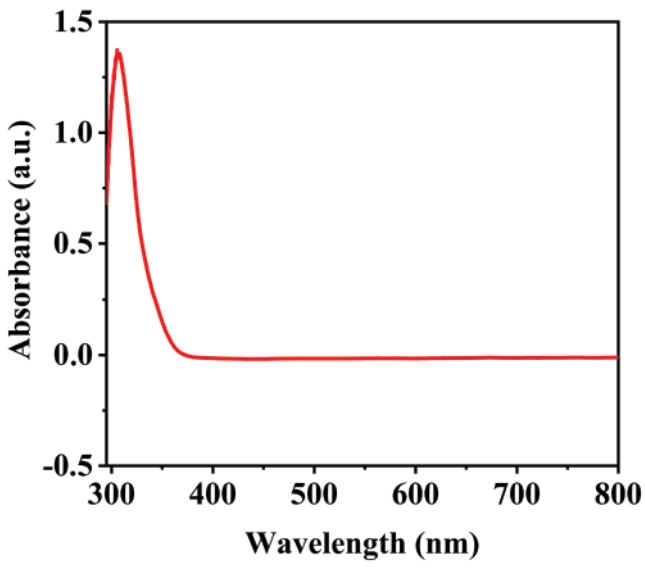

Fig. 4. Electronic absorption spectrum of compound **1a**.

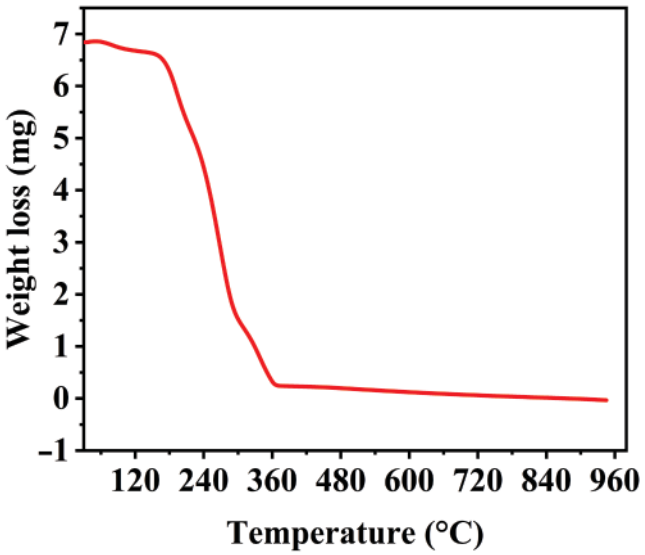

Fig. 5. TGA curve for compound **1a**.

bonds and decomposition of the aromatic ring and hydrazone fragment, and the weight loss amounts to ~5.5 mg. Almost no further weight loss was observed above 360°C, indicating complete thermal decomposition (Fig. 5). Thus, the results of thermal analysis demonstrate moderate thermal stability of compound **1a** (up to 230°C), so that the conditions of its application are limited by that temperature threshold.

We also performed DFT quantum chemical calculations of compound **1a**. Geometry optimization, determination of physicochemical characteristics, and data processing and visualization were done with the aid of Gaussian 16W and Avogadro. The structures of the highest occupied molecular orbital (HOMO) and lowest unoccupied molecular orbital (LUMO) of acetylhydrazone **1a** are shown in Fig. 6.

The HOMO is localized on the hydrazone fragment, which suggests nucleophilic nature of atoms therein. The LUMO is localized on the anilide group, which confirms its electron-withdrawing character. Thus, HOMO/LUMO analysis predicts the electronic properties of different molecular fragments and potential centers for complexation reactions and nucleophilic/electrophilic interactions.

The structure of acetoacetanilide acetylhydrazone (**1a**) was unambiguously determined by X-ray analysis of its single crystal (Fig. 7). Compound **1a** crystallized in space group *P*-1 belonging to the triclinic crystal system. The stable crystal packing of compound **1a** is determined by the system of N–H···O and N–H···N intermolecular hydrogen bonds and possible π-stacking interactions between the aromatic rings (judging by the close position of molecules along the *b* and *c* crystallographic axes. The geometric parameters of molecule **1a** (e.g., bond lengths, C=O ~1.22 Å, N–N ~1.39 Å and bond angle $N^1N^2C^{10}$ ≈ 117.7°) are consistent with the standard values for conjugated hydrazone systems. Molecules of **1a** in crystal are oriented as chains or layers stabilized by N–H···O hydrogen bonds, which emphasizes the potential of **1a** as ligand in coordination chemistry. The unit cell parameters are as follows: a = 4.7692(19), b = 8.433(4), c = 15.808(7) Å; α = 103.59(2)°, β = 94.795(19)°, γ = 96.60(2)°; V = 609.8(5) Å³; Z = 2.

Molecule **1a** has a nonplanar conformation where the acetyl and phenyl substituents are distant from each other. The hydrazone moiety and carbonyl group form a π-conjugated system, which could favor intra- and intermolecular interactions. The antiparallel orientation of dipoles reduces electrostatic repulsion. The calculated density is 1.390 g/cm³, which is typical of organic compounds with medium-sized molecules. The packing coefficient is fairly high for the triclinic system, indicating a compact packing. The side chain (butanamide fragment) has a bent conformation which

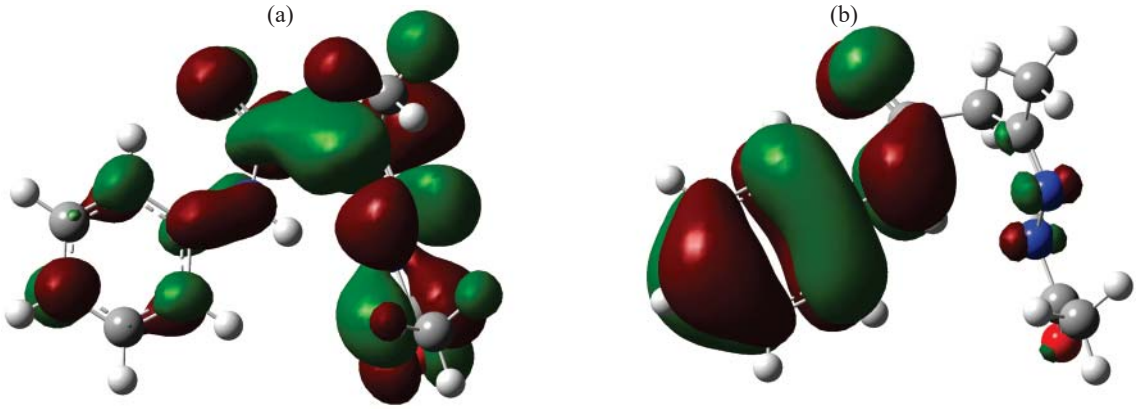

Fig. 6. Structures of the (a) (HOMO) and (b) LUMO of compound **1a** determined by DFT calculations.

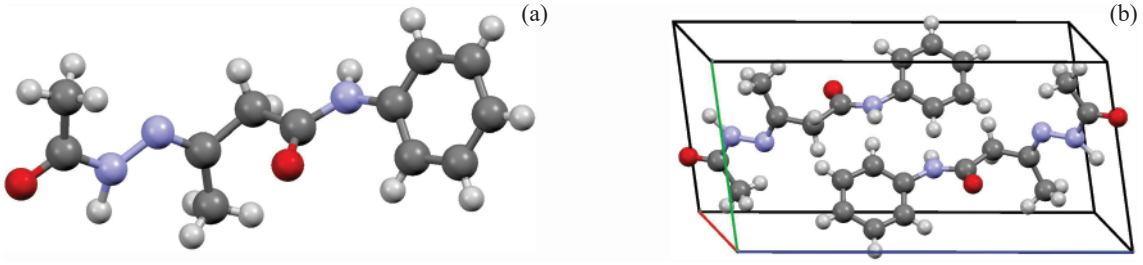

Fig. 7. (a) Molecular structure and (b) crystal packing of acetoacetanilide acetylhydrazone (**1a**).

facilitates intermolecular interactions. The final divergence factors were R = 0.098, $wR(F^2)$ = 0.267; goodness of fit S = 1.12; such values are acceptable for structures forming nonideal crystals, especially in the triclinic crystal system.

Based on the crystallographic data, we then performed Hirshfeld surface analysis of acetoacetanilide acetylhydrazone (**1a**) using Crystal Explorer21 [19]. The obtained two-dimensional fingerprint plots demonstrated percent contributions of different intermolecular interactions in crystal. We also calculated fractions of interatomic contacts visualized in these plots. The largest fraction corresponds to intramolecular (H–H 54,5%) and intermolecular (H–All 72,5%) hydrogen bonds. The smallest fractions were found for the interactions C–O (0%), N–C (1.1%), N–O (0.7%), N–N (0%), and O–O (0%) (Table 1).

EXPERIMENTAL

All reagents of analytical or chemically pure grade were used without further purification. Acetoacetanilide and acetylhydrazine were purchased from Sigma–Aldrich (USA). Ethanol (96%), acetic acid, *N*,*N*-dimethylformamide (DMF) and other solvents were purified according to standard procedures. The progress of the reaction was monitored by TLC on silica gel. The melting point was measured with an Electrothermal IA9100 melting point apparatus (UK). The elemental composition was determined from the high-resolution mass spectrum which was obtained with a Perkin Elmer NexION 2000 inductively coupled plasma mass-spectrometer (USA). The IR spectrum was recorded in the range of 4000–400 cm^{-1} on a Shimadzu IRTracer-100 FTIR spectrometer (Japan) from a sample prepared as KBr disk. The electronic absorption spectrum (λ 190–1000 nm) was measured in anhydrous ethanol on a Shimadzu UV-1900 spectrophotometer (Japan) using a 10-mm path length cell; concentration $c = 10^{-5}$ M.

(*E*)-3-(2-Acetylhydrazinylidene)-*N*-phenylbutanamide (1a). A 500-mL round-bottom flask was charged with 0.01 mol (1.77 g) of acetoacetanilide, and 100 mL of anhydrous ethanol was added. A reflux condenser was attached to the flask, and the mixture was stirred at 30–40°C until it became homogeneous. Acetohydrazide, 0.01 mol (0.74 g), was then added, and the mixture was refluxed with stirring on a water bath for 3 h. After completion of the reaction, approximately 1/3 of the solvent was removed under reduced pressure,

Table 1. Interatomic interactions in molecule **1a** in the fingerprint region

Interaction	Contribution, %	Interaction	Contribution, %
C–All	11.2	H–O	9.7
C–C	1.6	N–C	1.1
C–H	8.5	N–H	2.8
C–N	1.1	N–N	0
C–O	0.0	N–O	0.7
H–All	72.5	O-All	11.7
H–C	6	O–C	0
H–H	54.5	O–H	11.2
H–N	2.3	O–N	0.5

and the precipitate was filtered off, washed with cold ethanol, and dried at room temperature. Yield 1.864 g (80%), light yellow needles, mp 180°C. Found, %: C 61.14; H 6.31; N 17.92. $C_{12}H_{15}N_3O_2$. Calculated, %: C 61.79; H 6.48; N 18.01.

CONCLUSIONS

Acetoacetanilide acetylhydrazone has been synthesized by the condensation of acetoacetanilide and acetohydrazide. It is a stable compound, which was characterized by spectroscopic methods, scanning electron microscopy, thermogravimetric analysis, and X-ray diffraction data. The synthesized compound exists mainly in the hydrazone (imino) form and is potentially capable of coordinating and chelating metal ions. The new ligand can find application in antitumor therapy and bioimaging.

FUNDING

This work was supported by ongoing institutional funding. No additional grants to carry out or direct this particular research were obtained.

CONFLICT OF INTEREST

The authors declare that they have no conflicts of interest.

SUPPLEMENTARY INFORMATION

The online version contains supplementary material available at https://doi.org/10.1134/S1070428025603012.

REFERENCES

1. Vogel, A.I., *Textbook of Practical Organic Chemistry*, London: Longman Scientific & Technical, 1989, 5th ed.
2. Bhat, M.A., Khan, I.A., Ganaie, S.A., Pandith, A.H., and Hussain, M.K., *J. Mol. Struct*., 2020, vol. 1203, article ID: 127419. https://doi.org/10.1016/j.molstruc.2019.127419
3. Kargar, H. and Kia, R., *Polyhedron*, 2018, vol. 146, p. 134. https://doi.org/10.1016/j.poly.2018.03.055
4. Sharma, R., Bansal, A., Gupta, V.K., Mangal, M., and Kumar, P., *Spectrochim. Acta, Part A*, 2021, vol. 248, article ID: 119184. https://doi.org/10.1016/j.saa.2020.119184
5. Khalil, M.M.H., *J. Chem. Res*., 2017, vol. 41, no. 4, p. 221. https://doi.org/10.3184/174751917X14872598908884
6. Gök, Y., Eren, H., Tümer, M., and Demirtaş, İ., *J. Coord. Chem*., 2016, vol. 69, no. 6, p. 872. https://doi.org/10.1080/00958972.2016.1141431
7. Mishra, A., Kumar, A., Srivastava, S., Agarwal, V., and Shukla, G., *Eur. J. Med. Chem*., 2020, vol. 190, article ID: 112168. https://doi.org/10.1016/j.ejmech.2020.112168
8. Dharmendra, K., Meena, R., Soni, R., Sharma, A., Gupta, V., and Patel, R., *Bioorg. Med. Chem*., 2019, vol. 27, no. 4, p. 669. https://doi.org/10.1016/j.bmc.2019.02.004
9. Sutradhar, M. and Costa Pessoa, J., *Inorg. Chim. Acta*, 2018, vol. 470, p. 12. https://doi.org/10.1016/j.ica.2017.09.036
10. Mohamed, G.G., Omar, M.M., and Ibrahim A.A., *Spectrochim. Acta, Part A*, 2010, vol. 75, p. 678. https://doi.org/10.1016/j.saa.2009.11.039
11. Popioiek, Ł., Stefanska, J., Kielczykowska, M., Korolczuk, M., and Biernasiuk, A., *J. Heterocycl. Chem*., 2016, vol. 53, no. 2, p. 393. https://doi.org/10.1002/jhet.2392
12. Verma, G., Marella, A., Shaquiquzzaman, M., Akhtar, M., Ali, M.R., and Alam, M.M., *J. Pharm. Bioallied Sci*., 2014, vol. 6, no. 2, p. 69. https://doi.org/10.4103/0975-7406.129170
13. Gao, P. and Wei, Y., *Heterocycl. Commun*., 2013, vol. 19, no. 2, p. 113. https://doi.org/10.1515/hc-2012-0179
14. Rollas, S. and Küçükgüzel, S.G., *Molecules*, 2007, vol. 12, no. 8, p. 1910. https://doi.org/10.3390/12081910
15. Adiguzel, R., Ergin, Z., and Sekerci, M., *Asian J. Chem*., 2010, vol. 22, no. 5, p. 3895.
16. Tursunov, M.A., Umarov, B.B., and Avezov, K.G., *Moscow Univ. Chem. Bull*., 2019, vol. 74, p. 138. https://doi.org/10.3103/S0027131419030118
17. Becke, A.D., *Phys. Rev. A*, 1988, vol. 38, no. 6, p. 3098. https://doi.org/10.1103/PhysRevA.38.3098
18. Hanwell, M.D., Curtis, D.E., Lonie, D.C., Vandermeersch, T., Zurek, E., and Hutchison, G.R., *J. Cheminf*., 2012, vol. 4, p. 17. https://doi.org/10.1186/1758-2946-4-17
19. Spackman, M.A., Turner, M.J., McKinnon, J.J., Wolff, S.K., Grimwood, D.J., and Jayatilaka, D., CrystalExplorer21. Univ. Western Australia, 2021. https://crystalexplorer.net/